



HAL
open science

The Lorenz model for single-mode homogeneously broadened laser: analytical determination of the unpredictable zone

Samia Ayadi, Olivier Haeberlé

► **To cite this version:**

Samia Ayadi, Olivier Haeberlé. The Lorenz model for single-mode homogeneously broadened laser: analytical determination of the unpredictable zone. *Central European Journal of Physics*, 2014, 12 (3), pp.203-214. 10.2478/s11534-014-0440-4. hal-00998065

HAL Id: hal-00998065

<https://hal.science/hal-00998065>

Submitted on 30 May 2014

HAL is a multi-disciplinary open access archive for the deposit and dissemination of scientific research documents, whether they are published or not. The documents may come from teaching and research institutions in France or abroad, or from public or private research centers.

L'archive ouverte pluridisciplinaire **HAL**, est destinée au dépôt et à la diffusion de documents scientifiques de niveau recherche, publiés ou non, émanant des établissements d'enseignement et de recherche français ou étrangers, des laboratoires publics ou privés.

The Lorenz model for single-mode homogeneously broadened laser: analytical determination of the unpredictable zone

Research Article

Samia Ayadi^{1*}, Olivier Haeberlé^{2†}

1 Faculté de physique, Laboratoire d'électronique quantique, USTHB, Bp N 32 El Alia Bab Ezzouar ,16111 Alger,Algeria

2 Laboratoire MIPS EA2332, Université de Haute-Alsace, 61 rue Albert Camus, 68093 Mulhouse, France

Abstract: We have applied harmonic expansion to derive an analytical solution for the Lorenz-Haken equations. This method is used to describe the regular and periodic self-pulsing regime of the single mode homogeneously broadened laser. These periodic solutions emerge when the ratio of the population decay rate φ is smaller than 0.11. We have also demonstrated the tendency of the Lorenz-Haken dissipative system to behave periodic for a characteristic pumping rate $2C_P$ [7], close to the second laser threshold $2C_{2th}$ (threshold of instability). When the pumping parameter $2C$ increases, the laser undergoes a period doubling sequence. This cascade of period doubling leads towards chaos. We study this type of solutions and indicate the zone of the control parameters for which the system undergoes irregular pulsing solutions. We had previously applied this analytical procedure to derive the amplitude of the first, third and fifth order harmonics for the laser-field expansion [7, 17]. In this work, we extend this method in the aim of obtaining the higher harmonics. We show that this iterative method is indeed limited to the fifth order, and that above, the obtained analytical solution diverges from the numerical direct resolution of the equations.

PACS (2008): 42.55.-f, 42.55.Ah, 05.45.Pq

Keywords: Laser instabilities • Lorenz-Haken equations • Self-pulsing • Chaos.

© xxxxxxxx

1. Introduction

The simplest laser model is a single mode unidirectional ring laser containing a homogeneously-broadened, two-level medium, commonly designated as the Lorenz-Haken model. In 1975, Haken [1] showed equivalence between the Lorenz model that describes fluid turbulence [2], already known for leading to deterministic chaos, and the equations of a homogeneously-broadened, single-mode laser. In this context, such a laser can be viewed as a system, which becomes unstable under suitable conditions related to the respective values of the decay rate (bad

* E-mail: samia_ay@yahoo.com

† E-mail: olivier.haeberle@uha.fr

cavity condition) and of the level of excitation (second laser threshold). The numerical integration of the Lorenz-Haken model has indicated that the system undergoes a transition from a stable continuous wave output to a regular pulsing state. However, it also sometimes develops irregular pulsations (chaotic solutions). The nature of such irregular solutions was explained by Haken [1]. For more than thirty years, the approach towards solving Haken-Lorenz equations was dominated by the general line of thought that "the pulsing solutions of the single-mode laser equations must be found with numerical integration". Bougoffa and Bougouffa [3–5] presented an analytical approach based on Adomian decomposition to find the solutions of the Lorenz system. Their method was applied to find the stationary states. In a previous work [6, 7], it was shown that a simple harmonic expansion method permits to obtain analytical solutions for the laser equations, for physical situations where the long-term signal consists of regular pulse trains (periodic solutions). The corresponding laser field oscillates around a zero mean-value. In particular, we have shown that the inclusion of the third-order harmonic term in the field expansion allows for the prediction of the pulsing frequencies. The analytical expression of pulsing frequencies excellently matches their numerical counterparts, when the solution consists of regular period-one pulse trains. We have also derived a natural frequency, typical of the permanent pulsing-regime of operation. The aim of the present work is first to extract analytical information about the zone of period doubling and about the chaotic region, from the third-order expansion analysis. Then, the validity of the analytical development is discussed. We demonstrate in particular that the analytical expression of the periodic solutions diverges from the numerical one if one extends the development above the fifth order.

2. Haken-Lorenz equations: period-one oscillations

The model we start from is based on the Maxwell-Bloch equations in single mode approximation, considering a unidirectional ring laser containing a homogeneously broadened medium. The equations of motion are derived using a semi-classical approach, considering the resonant field inside the laser cavity as a macroscopic variable interacting with a two-level system. Assuming exact resonance between the atomic line and the cavity mode, and after adequate approximations, one obtains three coupled non-linear differential equations for the field, polarization, and population inversion of the medium, the so-called Lorenz-Haken model [8, 14, 16]:

$$\frac{dE(t)}{dt} = -\kappa \{E(t) + 2CP(t)\} \quad (1a)$$

$$\frac{dP(t)}{dt} = -P(t) + E(t)D(t) \quad (1b)$$

$$\frac{dD(t)}{dt} = -\varphi \{D(t) + 1 + P(t)E(t)\} \quad (1c)$$

where $E(t)$ represents the electric field in the laser cavity having a decay constant κ , $P(t)$ is the polarization of this field, $D(t)$ is the population difference having a decay constant φ . Both κ and φ are scaled with respect to the polarization relaxation rate, and $2C$ is the pump rate required for obtaining the lasing effect. To obtain the

steady-state solution of system (1), all derivatives with respect to time are set to zero. Under suitable conditions, the steady-state solution becomes unstable. We can delimit the boundary regime where Eqs. (1) involve unstable solutions by linear stability analysis (LSA) [8, 9]. This analysis leads to the following results: the loss of stability simultaneously requires a bad cavity (i.e., κ being sufficiently larger than $\wp + 1$) and a pumping parameter $2C$ larger than $2C_{2th}$ (the instability threshold condition). This threshold $2C_{2th}$ corresponds to the onset of instability and is given by:

$$2C_{th} = 1 + \frac{(\kappa + 1) (\kappa + 1 + \wp)}{(\kappa - 1 - \wp)} \quad (2)$$

At this critical value of the excitation parameter, the solution undergoes a subcritical Hopf bifurcation [10] and loses stability, leading to a large-amplitude, pulsing solution. We have solved numerically Eqs. (1) using a Runge-Kutta method with an adaptive integration step, and with the following parameters $\kappa = 3$, $\wp = 0.1$ and $2C = 10 > 2C_{th}$ ($2C_{2th} = 9.63$). The field and polarization oscillate around a zero mean-value, while the population inversion oscillates with a dc component. The corresponding frequency spectra obtained by Fast Fourier Transform (FFT) exhibit odd components at $\Delta, 3\Delta, 5\Delta, \dots$ for the field and polarization. On the contrary, the population inversion spectrum exhibits even components at $2\Delta, 4\Delta, 6\Delta, \dots$. These properties are at the basis of the strong-harmonic expansion method [6, 7, 13] that we use to construct analytical solutions. We now give a brief outline of the main steps of the adapted strong-harmonic expansion method we use. This yields analytical expressions for the angular frequency of the periodic solutions and for the first harmonics of the corresponding analytical solutions.

3. Iterative harmonic expansion

We here briefly summarize the analytical procedure, which we use to determine the long-term frequencies and amplitudes of the first harmonics of the field $E(t)$ [6, 7, 13]. We write the interacting variables as the following expansions:

$$E(t) = \sum_{n \geq 0} E_{2n+1} \cos((2n+1)\Delta t) \quad (3a)$$

$$P(t) = \sum_{n \geq 0} P_{2n+1} \cos((2n+1)\Delta t) + P_{2n+2} \sin((2n+1)\Delta t) \quad (3b)$$

$$D(t) = D_0 + \sum_{n \geq 0} D_{2n+1} \cos((2n+2)\Delta t) + D_{2n+2} \sin((2n+2)\Delta t) \quad (3c)$$

Limiting these expansions to the third order for the field and polarization, and to the second order for the population inversion in Eqs. (3), we obtain the expression of the angular frequency of the pulsating solution [6, 7]:

$$\Delta^2 = \frac{(2C - 1) \kappa \wp (2 + \wp) - 3 (\kappa + 1) \wp^2}{8 (\kappa + 1) - \wp (2\kappa + \wp + 4)} \quad (4)$$

The details of these calculations are given in section 2 and appendix A of Ref. [7]. This formula shows dependence to the pumping parameter $2C$ and indicates that the frequency of the signal increases with the excitation level. We have previously [6] proved that the analytical frequency given by Eq. (4) perfectly matches the frequency numerically derived from Eqs. (1). Another expression for the operating long-term frequency [7] is obtained:

$$\Delta_p = \sqrt{\frac{3\varphi + 2\kappa(1 + 2\varphi)}{24 + 6\kappa + 9\varphi}} \quad (5)$$

This expression shows no dependence to the excitation level $2C$. It constitutes an expression of the natural frequency that characterizes a given set of κ and φ values that allow for periodic solutions. This frequency will be used to delimit the domain where the laser exhibits regular oscillations.

4. Chaos via a period doubling sequence

A. Narducci *et al.* [14, 15] have shown that parameter φ plays an important role in defining the kind of dynamics predicted by the Lorenz-Haken model. Numerical simulations [13] with $\kappa = 3$ and $\varphi = 0.1$ (Fig. 1) have shown that large-amplitude periodic solutions dominate over the range $10 < 2C < 32$. The behaviour of these periodic solutions for increasing gain $2C$ is extremely variable.

First, the laser displays a symmetric and period-one solution (Fig. (1a)). This solution has been called symmetrical because of the symmetry of $E(t)$ with respect to $E = 0$: the projection of the trajectory onto the (E, D) plane produces symmetrical loops as shown in Fig. (1b). For increasing excitation level $2C$ ($2C = 18.4$), the previously symmetric, period-one solution becomes asymmetric. The field amplitude undergoes a symmetry-breaking transformation with different positive and negative excursions (Figs. (1c,1d)). For $2C = 29$, the laser exhibits a period-two, asymmetric solution (Figs. (1e,1f)). This feature corresponds to the period-doubling bifurcations. These results illustrate that period-doubling bifurcations can only emerge from asymmetrical solutions, as shown by Swift and Weisenfeld [18]. As the excitation level further increases, more and more complicated patterns emerge, which eventually lead to chaotic behaviour. As shown in Figs. (1g,1h) and Figs. (1i,1j), the temporal trace of the field exhibits asymmetric solution with period four when $2C = 29.7$, and finally becomes chaotic for $2C = 32$.

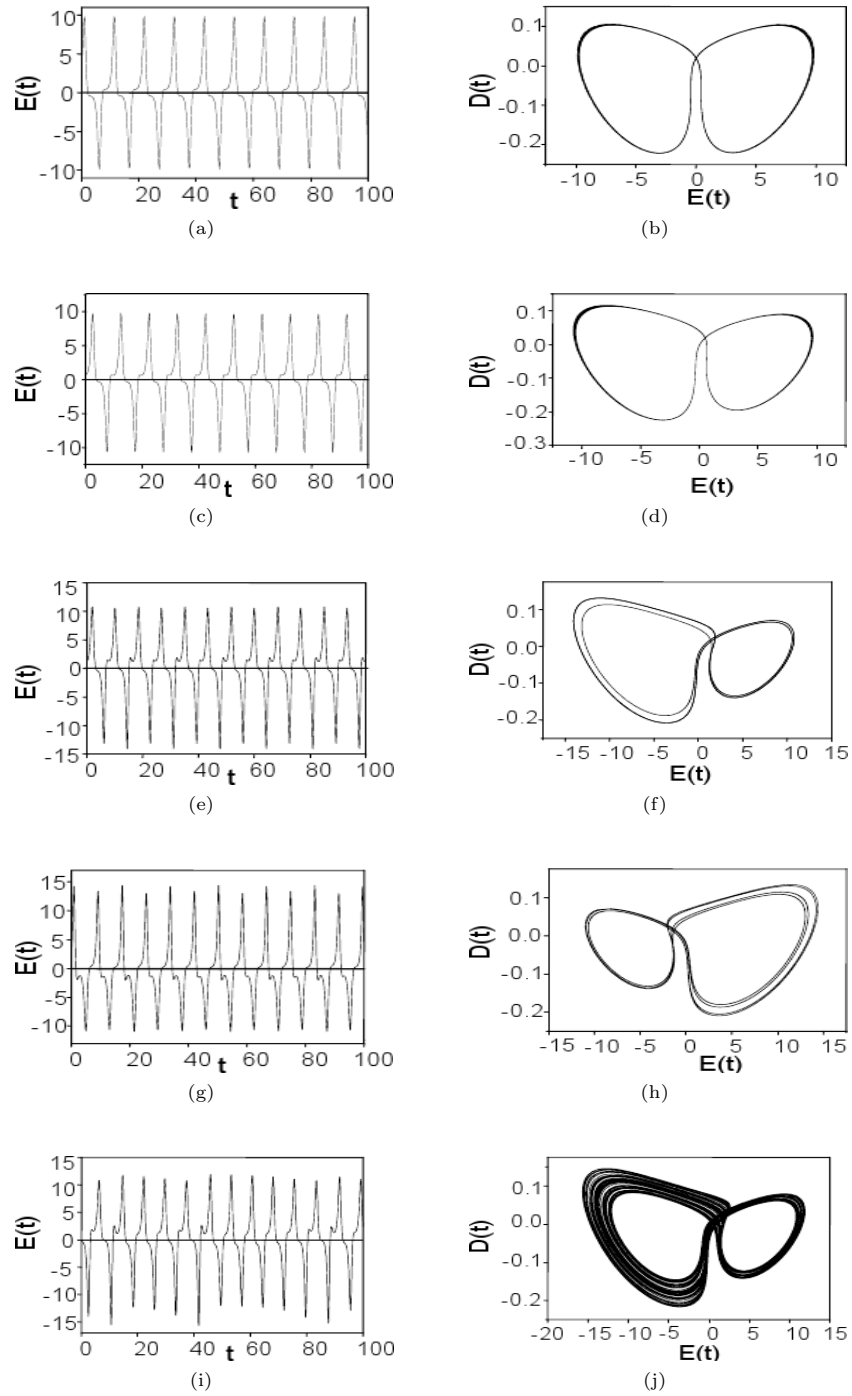


Figure 1: Examples of Eqs. (4) solutions for $(\kappa = 3, \varphi = 0.1)$. Left column: time dependence of the electric field amplitude. a) Symmetric solution with period one, obtained with $2C = 18.4$. b) Asymmetric, period-one solution, obtained with $2C = 20$. c) Asymmetric solution with period two, obtained with $2C = 29$. d) Asymmetric solution with period four, obtained with $2C = 29.7$. e) Chaotic solution. Right column: attractor projection onto the (D, E) -plane. One can distinguish a cascade of period doublings, which leads to chaos.

We now attempt to delimit the zone where the laser can exhibit periodic pulsations using the analytical method. At first, we derive the analytical expression of the pumping rate $2C$ that leads the laser to oscillate with period one, period two and over. To get this expression, we assume that the pulsation frequency Eq. (4) is proportional to the eigenfrequency Eq. (5):

$$\Delta = \alpha \Delta_p \quad (6)$$

α being a rational number. Then, $2C_\alpha$ takes the following form:

$$2C_\alpha = \frac{(2k + 3\wp + 4\kappa\wp) \{ \alpha^2 [8(\kappa + 1) - \wp(2\kappa + \wp + 4)] + 3\wp(8 + 2\kappa + 3\wp) \}}{3\kappa\wp(2 + \wp)(8 + 2\kappa + 3\wp)} \quad (7)$$

For different values of α , we get the pumping level $2C_\alpha$ that we have used for numerically solving Eqs. (1). These numerical solutions for the chosen parameters $\kappa = 3$ and $\wp = 0.1$ can be categorized into four classes, depending on the values of α :

Symmetric and period-one solutions:	$1 \leq \alpha < 1.5$ ($9.63 \leq 2C \leq 18.4$)
Asymmetric solutions with period one:	$\alpha \leq 1.75$ ($18.4 < 2C \leq 27.8$)
Asymmetric solutions with period two and over:	$1.75 < \alpha < 2$ ($27.9 \leq 2C < 32$)
Chaotic solutions:	$\alpha \geq 2$ ($2C > 32$)

These results are illustrated in Fig. (1), and the route to chaos via period doubling is clearly identified. We conclude that the chaotic behaviour takes place for $\alpha \geq 2$. This last result allows for delimiting the region of control parameters where the operation of the homogeneously-broadened single mode laser can be chaotic. To do so, we assume that $2C_{2th}$ is equal to $2C_2$. From this identity, we derive a characteristic equation of \wp according to κ :

$$64\kappa - 64\kappa^3 + (96 + 208\kappa + 92\kappa^2 - 40\kappa^3 + 12\kappa^4)\wp + (120 + 242\kappa + 274\kappa^2 + 70\kappa^3 + 6\kappa^4)\wp^2 + (24 + 41\kappa + 76\kappa^2 - 5\kappa^3)\wp^3 + (15\kappa + 29\kappa^2)\wp^4 = 0 \quad (8)$$

We have solved Eq. (8) using the Mathematica™ software to found the analytical expressions of its roots. Accepting only solutions with physical meaning (\wp positive), we obtain the curve illustrated in Fig. (2a). This curve separates the periodic-solution zone (an example of periodic solution being depicted in Fig. (2b)), the so-called predictable zone, from the chaotic-operation zone (an example of chaotic solution being depicted in Fig. (2c)). This region is called the unpredictable zone, characterized by $2C_2 > 2C_{2th}$.

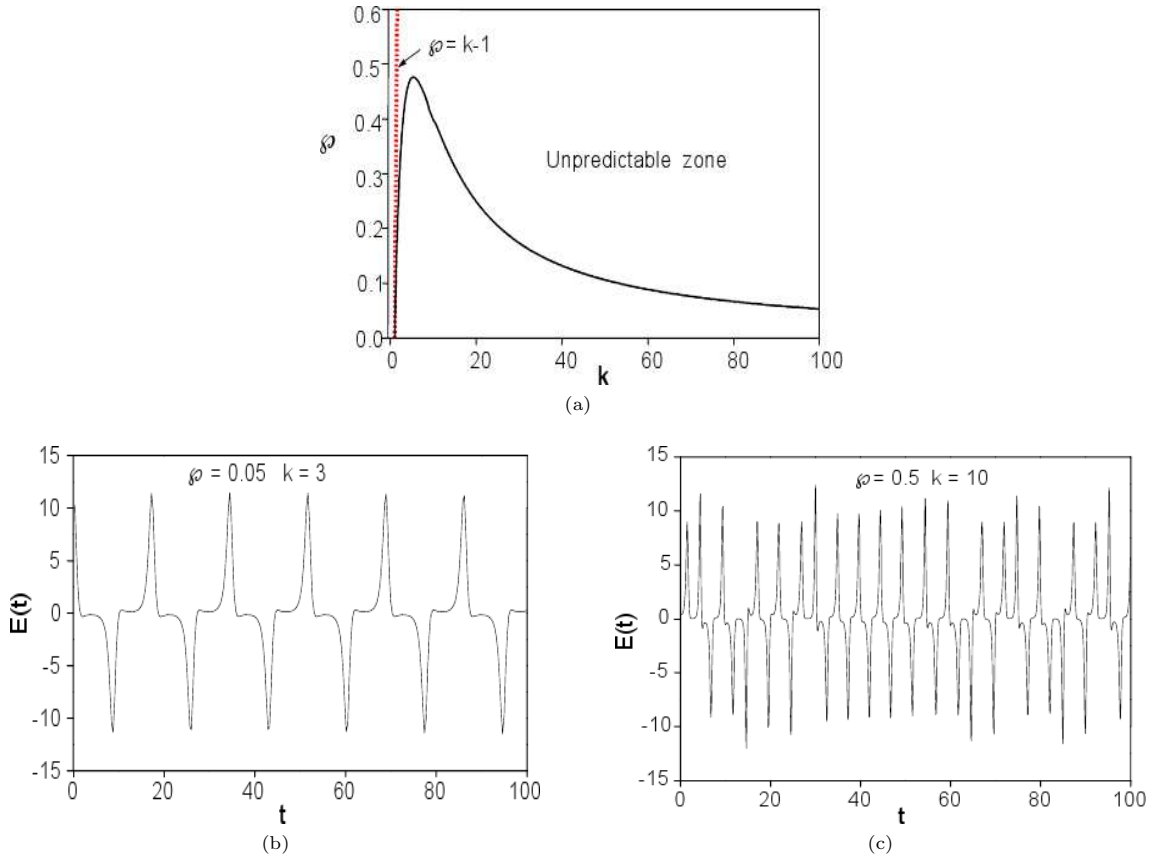


Figure 2: a) Predictable and unpredictable zone. b) Example of periodic solution in the region $C_2 < C_{2th}$.
c) Example of chaotic pulsation for $C_2 > C_{2th}$.

5. Analytical periodic solutions

The analytical development described in section 3 permits to establish the analytical expression of the electric field. This was done in a previous work (see appendix A in Ref. [7]) to derive the expressions of the first and third-order harmonics of the field:

$$E_1 = -2CP_1 = \frac{2\sqrt{(1+\Delta^2)(4\Delta^2+\varphi^2)(1+\kappa)}}{\sqrt{\varphi}\sqrt{(\varphi+2\kappa+2\varphi\kappa-\Delta^2(4+\varphi+2\kappa))}} \quad (9)$$

$$E_3 = -2CP_3 = -\frac{T_{3d}(\varphi^2(1-3\Delta^2)-8\varphi\Delta^2)\frac{E_1^3}{4}}{1-T_{1d}(\varphi^2(1-\Delta^2)-4\varphi\Delta^2)\frac{E_1^2}{4}} \quad (10)$$

The expressions of E_1 and E_3 are related to the decay rates φ and κ , and to the excitation parameter $2C$ through their dependence on the pulsing frequency Δ . Using the previously described analytical features, we now construct

a typical sequence of analytical solutions being the counterparts of the numerical one, presented on Fig. (3a). The long term operating frequency is estimated from Eq. (4), while the first and third order field components are evaluated from Eqs. (9) and (10), respectively. The values of these components, for $\kappa = 3$, $\wp = 0.1$ and $2C = 10$, are $E_1 = 5.19$ and $E_3 = 1.72$ and the corresponding frequency is $\Delta = 0.42$. Thus, to the third order, the analytical field expansion takes the following form:

$$E(t) = 5.19 \cos(0.42 t) + 1.72 \cos(3 \times 0.42 t) \quad (11)$$

The temporal evolution of Eq. (11) is illustrated in Fig. (3b). One may notice the resemblance with its numerical counterpart depicted in Fig. (3a), however, differences remain between the analytical and the numerical solutions. The pulses peak at $E_n = 7.75$ in the long-term time trace of Fig. (3a), while from the analytical solution expressed by Eq. (11) we find $E \approx 6.95$. This difference can be attributed to the limitation of a third-order-only development. To verify this hypothesis, we have extended the calculations towards fifth order in field amplitude [13, 17]. Hence, we expand Eqs. (3) to fifth order (for $n = 2$) for the electric field and polarization and adopt the same procedure as in section 3. After calculations, we obtain the fifth components in terms of the first and the third order field amplitudes:

$$P_5 = \Gamma_d \Gamma_5 \{ f E_1^5 + g E_1^2 E_3 + h E_1^4 E_3 + q E_1 E_3^2 + s E_1^3 E_3^2 \} \quad (12)$$

$$E_5 = -2CP_5 = -2C\Gamma_d \Gamma_5 \{ f E_1^5 + h E_3 E_1^4 + s E_3^2 E_1^3 + g E_3 E_1^2 + q E_3^2 E_1 \} \quad (13)$$

The parameters Γ_d , Γ_5 , and the weight functions f , g , h , q and s , are written as:

$$f = -\frac{1}{16} T_{3d} \Gamma_4 \left(\frac{\wp \alpha_3}{4\Delta} - 2\wp \Delta \alpha_4 - 5\Delta \alpha_3 - \frac{5\wp^2 \Delta \alpha_4}{2} \right) \quad (14)$$

$$g = -\frac{1}{4} \left[\Gamma_4 \left(-\frac{\wp}{4\Delta} + 6\Delta + \frac{5\wp \Delta}{4} \right) + \Gamma_2 \left(-\frac{\wp}{4\Delta} + 6\Delta + \frac{5\wp \Delta}{4} \right) \right] \quad (15)$$

$$h = \frac{1}{16} \begin{bmatrix} -\Gamma_4 T_{1d} \left(\frac{\wp \alpha_1}{4\Delta} - 2\wp \Delta \alpha_2 - 5\Delta \alpha_1 - \frac{5\wp^2 \Delta \alpha_2}{2} \right) \\ -\Gamma_2 T_{1d} \alpha_1 \left(-5\Delta + \frac{\wp}{2\Delta} \right) + 2\Gamma_2 T_{1d} \alpha_2 \wp \Delta \left(1 + \frac{5\wp}{2} \right) \\ -\Gamma_2 T_{3d} \alpha_3 \left(-5\Delta + \frac{\wp}{2\Delta} \right) + 2\Gamma_2 T_{3d} \alpha_4 \wp \Delta \left(1 + \frac{5\wp}{2} \right) \end{bmatrix} \quad (16)$$

$$q = \Gamma_2 \left[\frac{\wp}{8\Delta} - \Delta + 5\Delta \frac{\wp}{8} \right] \quad (17)$$

$$s = \frac{1}{16} \left[-\Gamma_2 T_{1d} \left(\frac{\alpha_1 \wp}{2\Delta} + 2\wp \Delta \alpha_2 - 5\Delta (\alpha_1 - \alpha_2 \wp^2) \right) \right] \quad (18)$$

where:

$$\Gamma_2 = \frac{2\wp \Delta}{\wp^2 + 4\Delta^2}, \Gamma_4 = \frac{4\wp \Delta}{\wp^2 + 16\Delta^2}, \Gamma_5 = \frac{1}{1 + 25\Delta^2}, \Gamma_d = \frac{1}{1 + \Delta^2 + \frac{E_1^2}{2}} \quad (19)$$

$$T_{1d} = \frac{1}{(1 + \Delta^2)(\wp^2 + 4\Delta^2)}, T_{3d} = \frac{1}{(1 + 9\Delta^2)(\wp^2 + 4\Delta^2)} \quad (20)$$

$$\alpha_1 = \wp^2(1 - \Delta^2) - 4\wp \Delta^2, \alpha_2 = 1 + \wp - \Delta^2, \alpha_3 = \wp^2(1 - 3\Delta^2) - 8\wp \Delta^2, \alpha_4 = 1 + 2\wp - 3\Delta^2 \quad (21)$$

For $\kappa = 3$, $\wp = 0.1$ and $2C = 10$, we computed E_5 to get $E_5 = 1.23$. Thus, to the fifth order, the analytical field expansion writes as:

$$E(t) = 5.19 \cos(0.42t) + 1.72 \cos(3 \times 0.42t) + 1.23 \cos(5 \times 0.42t) \quad (22)$$

and is represented in Fig. (3c). Compared to the signal of Fig. (3a), the time trace of Fig. (3c) exhibits thinner and higher peaks, with values approaching those of their numerical counterpart in Fig. (3a). A priori, expanding Eqs. (3) to further higher orders should lead to an even better agreement between the numerical solution and the analytical expansion method we have adopted.

6. Higher order expansion

We therefore now extend the calculations above the fifth order. At first, we calculate the seventh-order components, by expanding the development in Eqs. (3) to $n = 3$ for the field and polarization, and inserting the obtained relations in Eqs. (1). The calculations are time-consuming but straightforward with the help of the Mathematica™ software, and one obtains the seventh-order component for the field in the form:

$$E_7 = -2C[W_7 E_1^7 + V_7 E_1^6 + F_7 E_1^5 + H_7 E_1^4 + S_7 E_1^3 + R_7 E_1^2 + Q_7 E_1 + Z_7] \quad (23)$$

The complete expressions of W_7 , V_7 , F_7 , H_7 , S_7 , R_7 , Q_7 and Z_7 are given in Appendix A, for the interested reader who would like to make use of these developments.

For $\kappa = 3$, $\wp = 0.1$, and $2C$, one obtains:

$$W_7 = 8.27 \times 10^{-9}, V_7 = 1.06 \times 10^{-5}, F_7 = 5.19 \times 10^{-5}, H_7 = 5.21 \times 10^{-4}, S_7 = 1.84 \times 10^{-3}, R_7 = -1.46 \times 10^{-2}, \\ Q_7 = -5.80 \times 10^{-2}, Z_7 = -3.64 \times 10^{-3}.$$

With these values, we obtain $E_7 = -3.70$. Therefore, the analytical field expansion is given by the expression:

$$E(t) = 5.19 \cos(0.42t) + 1.73 \cos(3 \times 0.42t) + 1.23 \cos(5 \times 0.42t) - 3.70 \cos(7 \times 0.42t) \quad (24)$$

The evolution of this expression against time is shown in Fig. (3d). We note that there still is a disagreement between Fig. (3a) and Fig. (3d), owing to the negative sign of the seventh component. To correct this variance, one should take into account higher order components in the analytical expression of the field. Analytical evaluation of the higher terms of the field is however very lengthy and tedious, so we propose to continue the evaluation in a semi-analytical, semi-numerical way. This implies that we inject the values of parameters κ , \wp and $2C$ in Eqs. (1) and Eqs. (3), and then evaluate the field components numerically by adopting the same procedure as before. The field spectra obtained by FFT exhibit components up to the 13th term. We therefore compute the

numerical components up to this order. For $\kappa = 3$, $\varphi = 0.1$ and $2C = 10$, such a procedure directly yields the higher-order terms:

$$E_9 = -64.97, \quad E_{11} = 1275.46 \quad \text{and} \quad E_{13} = 8.53 \times 10^9 \quad (25)$$

The field expansion then becomes:

$$E(t) = 5.19 \cos(0.42t) + 1.73 \cos(3 \times 0.42t) + 1.23 \cos(5 \times 0.42t) - 3.34 \cos(7 \times 0.42t) \\ - 64.97 \cos(9 \times 0.42t) + 12759.46 \cos(11 \times 0.42t) + 8.53 \cdot 10^9 \cos(13 \times 0.42t) \quad (26)$$

The time evolution of the expression given by Eq. (26) is represented in Fig. (3e). Discrepancies between this semi-analytical solution and the purely numerical one given on Fig. (3a) are still noticeable, while one expected indeed a better correspondance, thanks to the extended expansion. An attempt explanation for these remaining discrepancies is that they are in fact inherent to our procedure, which is iterative, based on the successive introduction of the orders of the electric field, order after order. For example, to find E_3 it is necessary to calculate E_1 (as E_3 depends on E_1), and similarly to have the value of E_5 , it is required to know the value of E_1 and E_3 (see Eq. (13)). As a consequence, the residual error on a specific term calculation increases with increasing term order, and ($E_{11} \gg E_1, E_{13} \gg E_1$), because the dependence of one term on the previous terms is non-linear. For example, E_5 shows a dependence on E_1 at the fifth power, and on E_3 at the second power. The Lorenz-Haken equations form a strongly nonlinear system, and therefore, little errors on the first terms are greatly amplified on the next terms, which explains that the analytical method will diverge from the numerical one.

This establishes the limit of the method: with the approach originally depicted in Refs. [6, 7, 13], expansion above the fifth order does not bring noticeable improvement to accuracy of the analytical expressions of the field. We however believe that one could obtain a better accuracy between the analytical and the numerical solution if developing Eqs. (3) up to the thirteenth order (as the field spectra obtained by FFT exhibit components up to the 13th term), taking into account all terms without truncation, and inserting the obtained expansion in the system of equations Eqs. (1). Future work will explore this hypothesis.

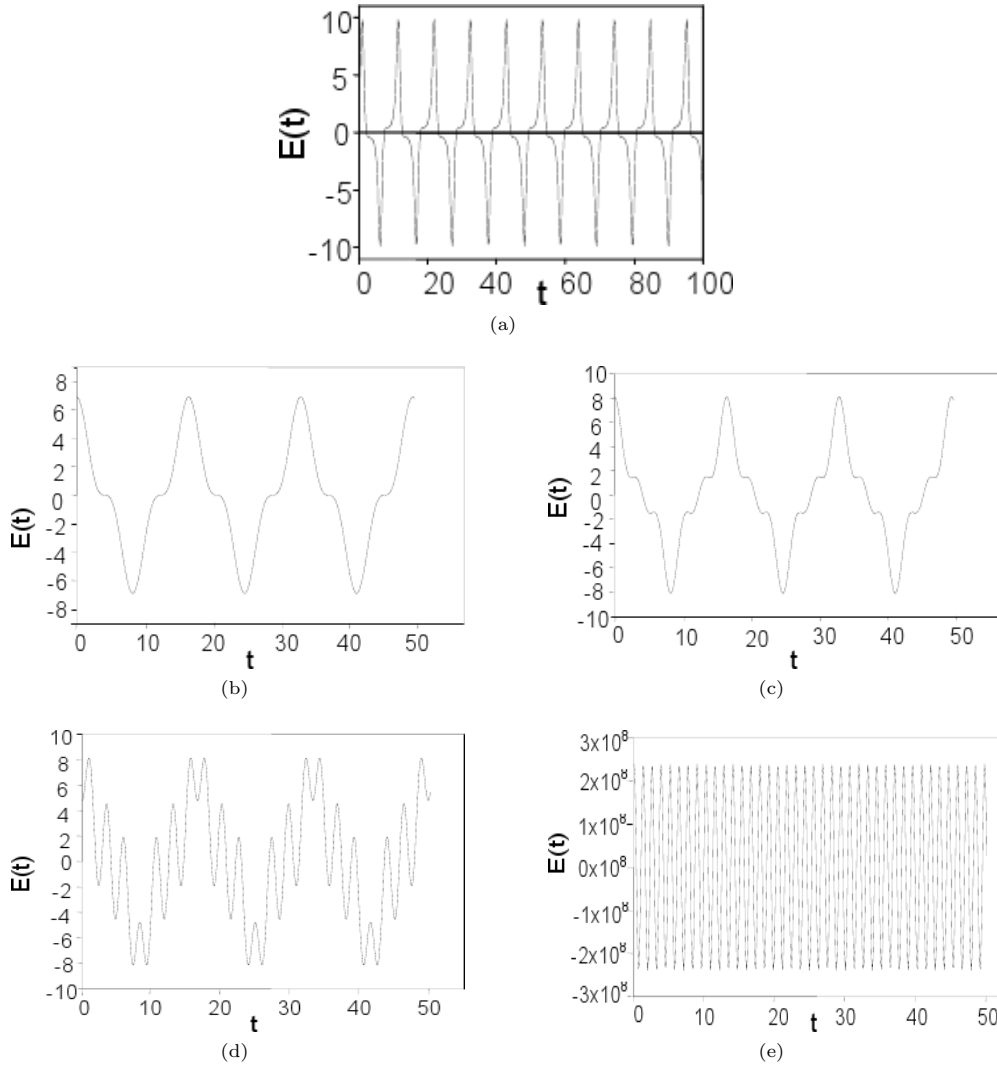


Figure 3: a) Long-term time dependence of the electric-field amplitude. Analytical solutions representation for b) third-order, c) fifth-order, d) seventh-order, and e) thirteenth-order for laser-field amplitude for $\kappa = 3$, $\varphi = 0.1$ and $2C = 10$.

7. Conclusion

We have expanded the analytical procedure, introduced in previous work [6, 7], that describes the self-pulsing regime of the single-mode homogeneously broadened laser operating in bad cavity configurations. The inclusion of the third-order harmonic term in the field expansion allows for deriving the analytical expression of the pumping rate $2C_\alpha$, that leads the laser to display period-doubling sequence. We have shown that for $\alpha < 2$, the dynamical

behaviour is periodic. It is important to note that constructing analytical or semi-analytical boundaries between the various periodic regions is not an easy task, because of the non-linear behaviour of the laser. Despite these difficulties, our method allows for a satisfactory localization of the periodic solution (predictable zone). We have also highlighted a divergence between the numerical solution and the analytical one when we extend the evaluation above the fifth order in the expression of the laser field. Analytical expansion is not meant to replace numerical integration of the Lorenz-Haken model, which is usually the preferred procedure, but development up to the third order gives accurate results, and may be used as an alternate to direct numerical solutions, with the advantage of greater ease of use. In that case, our approach may help to address the physics of laser chaos, especially for non-specialists. It is interesting to mention that the Lorenz equations represent a challenge, indexed by Smale [11, 12] in its list of the fourteen problems, which constitute, according to him, a serious challenge to mathematicians.

References

- [1] H. Haken, *Phys. Lett. A* 53, 77 (1975)
- [2] E. N. Lorenz, *J. Atmos. Science* 20, 130 (1963)
- [3] L. Bougouffa and S. Bougouffa, *Appl. Math. Comput.* 177, 553 (2006)
- [4] S. Bougouffa, *AIP Conf. Proc.* 1048, 109 (2008)
- [5] S. Bougouffa, S. Al-Awfi, and L. Bougouffa, *Appl. Math. Sciences* 1, 2917 (2007)
- [6] S. Ayadi and B. Meziane, *Opt. Quant. Elect.* 39, 51 (2007)
- [7] B. Meziane and S. Ayadi, *Opt. Comm.* 281, 4061 (2008)
- [8] H. Haken, *Light*, Vol. 2. (North-Holland Physics Publishing, 1985)
- [9] Ya. I. Khanin, *Fundamental of Laser Dynamics*. (Cambridge Int. Science Publ., 2006)
- [10] C. T. Sparrow, *The Lorenz Equation: Bifurcation, Chaos and Strange Attractors*. (Berlin Heidelberg:Springer-Verlag, 1982)
- [11] S. Smale, *Math. Intelligencer* 20, 7 (1998)
- [12] W. Tucker, *Found. Comput. Math.* 2, 53 (2002)
- [13] B. Meziane, *Atomic, Molecular and Optical Physics: New Research*, Nova Science Publisher, New York, 61 (2009)
- [14] L. M. Narducci, H. Sadiky, L. A. Lugiato, and N. B. Abraham, *Opt. Comm.* 55, 370 (1985)
- [15] L. M. Narducci and N. B. Abraham, *Laser physics and laser instabilities*. (World Scientific Publishing Co Pte Ltd, 1988)
- [16] R.G. Harrison and D. J. Biswas, *Prog. Quant. Electron* 10, 147 (1985)
- [17] S. Ayadi and B. Meziane, In *Semiconductor Lasers and Laser Dynamics III*. Proc. of SPIE Vol. 6997 (SPIE, Bellingham, WA, 69971D1-69971D9 2008).
- [18] J. W. Swift and K. Weisenfeld, *Phys. Rev. Lett.* 52, 705 (1984)

Appendix A: Derivation of the Seventh-Order Field Component

We give here the weight functions of the analytical expression of the electric field $E(t)$ at seventh order $E_7(t)$ given by Eq. (23). This expression have been derived from Eq. (3), expanded up to $n = 3$, inserting these equations into the Lorenz-Haken equations Eqs. (1a-1c) and identifying the same order-harmonic terms in each relation using the Mathematica™ software. We find a hierarchical set of algebraic relations:

$$P_1 = f_1 E_1^5 + h_1 E_1^4 + s_1 E_1^5 + r_1 E_1^2 + q_1 E_1 \quad (\text{A1})$$

$$P_2 = f_2 E_1^5 + h_2 E_1^4 + s_2 E_1^5 + r_2 E_1^2 + q_2 E_1 \quad (\text{A2})$$

$$P_3 = f_3 E_1^5 + h_3 E_1^4 + s_3 E_1^5 + r_3 E_1^2 + q_3 E_1 + z_3 \quad (\text{A3})$$

$$P_4 = f_4 E_1^5 + h_4 E_1^4 + s_4 E_1^5 + r_4 E_1^2 + q_4 E_1 + z_4 \quad (\text{A4})$$

$$P_5 = f_5 E_1^5 + h_5 E_1^4 + s_5 E_1^5 + r_5 E_1^2 + q_5 E_1 \quad (\text{A5})$$

$$P_6 = f_6 E_1^5 + h_6 E_1^4 + s_6 E_1^5 + r_6 E_1^2 + q_6 E_1 \quad (\text{A6})$$

$$P_7 = W_7 E_1^7 + V_7 E_1^6 + F_7 E_1^5 + H_7 E_1^4 + S_7 E_1^5 + R_7 E_1^2 + Q_7 E_1 + Z_7 \quad (\text{A7})$$

The seventh order field component is related to the first component through:

$$E_7 = -2C [P_7] = -2C [W_7 E_1^7 + V_7 E_1^6 + F_7 E_1^5 + H_7 E_1^4 + S_7 E_1^5 + R_7 E_1^2 + Q_7 E_1 + Z_7] \quad (\text{A8})$$

with:

$$W_7 = \Gamma_{10} \Gamma_7 \left[\frac{\wp^2}{2} (-f_5 + 7f_6 \Delta) + 3\wp \Delta (7f_5 \Delta + f_6) \right] \quad (\text{A9})$$

$$\begin{aligned} F_7 = & \Gamma_6 \Gamma_7 E_5 \left[\frac{\wp^2}{2} \left(-E_3 f_1 - E_5 f_3 - E_3 f_5 - h_1 - h_3 + 7\Delta \left(-E_3 f_2 - E_5 f_4 + E_3 f_6 + h_2 + h_4 \right) \right) \right. \\ & \left. + \wp \Delta \left(-E_3 f_2 - E_5 f_4 + E_3 f_6 + h_2 + h_4 + 7\Delta (E_3 f_1 + E_5 f_3 + E_3 f_5 + h_1 + h_3) \right) \right] \\ & + \Gamma_8 \Gamma_7 E_3 \left[\frac{\wp^2}{2} (-E_3 f_1 - E_5 f_1 - h_3 - h_5 + 7\Delta (E_3 f_2 - E_5 f_2 + h_4 + h_6)) \right. \\ & \left. + \wp \Delta (2(E_3 f_2 - E_5 f_2 + h_4 + h_6) + 14\Delta (E_3 f_1 + E_5 f_1 + h_3 + h_5)) \right] \\ & + \Gamma_{10} \Gamma_7 \left[\frac{\wp^2}{2} (-E_5 h_1 - 3E_3 - s_5 + 7\Delta (E_3 h_4 + s_6 + E_5 h_2)) \right. \\ & \left. + \wp \Delta (3E_3 h_4 + 3s_6 + 3\Delta (7E_5 h_1 + 7E_3 h_3 + 7s_5 \wp + E_5 h_2)) \right] \end{aligned} \quad (\text{A10})$$

$$\begin{aligned}
 V_7 = & \Gamma_6 \Gamma_7 E_5 \left[\frac{\wp^2}{2} (-f_1 - f_3 + 7\Delta (f_2 + f_4)) + \wp \Delta (f_2 + f_4 + 7\Delta (f_1 + f_3)) \right] \\
 & + \Gamma_{10} \Gamma_7 \left[\frac{\wp^2}{2} (-E_5 f_1 - E_3 f_3 - h_5 + 7\Delta (E_5 f_2 + E_3 f_4 + h_6)) \right. \\
 & \left. + \wp \Delta (3 (E_5 f_2 + E_3 f_4 + h_6) + 21\Delta (E_5 f_1 + E_3 f_3 + h_5)) \right] \tag{A11}
 \end{aligned}$$

$$\begin{aligned}
 & + \Gamma_8 \Gamma_7 E_3 \left[\frac{\wp^2}{2} (-f_3 - f_5 + 7\Delta (f_4 + f_6)) \right. \\
 & \left. + \wp \Delta (2 (f_4 + f_6) + 14\Delta (f_3 + f_5)) \right] \\
 Q_7 = & \Gamma_6 \Gamma_7 E_5 \left[\frac{\wp^2}{2} (-E_3 q_1 - E_3 q_5 - z_3 + 7\Delta (-E_3 q_6 - E_3 q_2 + z_4)) \right. \\
 & \left. + \wp \Delta (-E_3 q_2 + E_3 q_6 + z_4 + 7\Delta (z_3 + E_3 q_1 + E_3 q_5)) \right] \\
 & + \Gamma_8 \Gamma_7 E_3 \left[\frac{\wp^2}{2} (-z_3 - E_3 q_1 - E_5 q_1 + 7\Delta (z_4 + E_3 q_2 - E_5 q_2)) \right. \\
 & \left. + \wp \Delta (2 (E_3 q_2 - E_5 q_2 + z_4) + 14\Delta (E_3 q_1 + E_5 q_1 + z_3)) \right] \tag{A12} \\
 & + \Gamma_{10} \Gamma_7 E_3 \left[\frac{\wp^2}{2} (7 z_4 \Delta - z_3) + 3\wp \Delta (z_4 + 7 z_3 \Delta) \right]
 \end{aligned}$$

$$\begin{aligned}
 H_7 = & \Gamma_6 \Gamma_7 E_5 \left[\frac{\wp^2}{2} \begin{pmatrix} -E_3 h_1 - E_5 h_3 - E_3 h_5 - h_1 - s_3 + \\ 7\Delta (-E_3 h_2 + E_3 h_6 - E_5 h_4 + E_5 s_2 + s_4) \end{pmatrix} \right. \\
 & \left. + \wp \Delta \begin{pmatrix} s_4 - E_3 h_2 - E_5 h_4 + E_3 h_6 + s_2 + 7\Delta \\ (E_3 h_1 + s_1 + s_3 + E_5 h_3 + E_3 h_5) \end{pmatrix} \right] \\
 & + \Gamma_{10} \Gamma_7 \left[\frac{\wp^2}{2} (-r_5 - E_5 s_1 - E_3 s_3 + 7\Delta (E_5 s_2 + r_6 + E_3 s_4)) \right. \\
 & \left. + \wp \Delta (3 (r_6 + E_5 s_2 + E_3 s_4) + 21\Delta (r_5 + E_5 s_1 + E_3 s_3)) \right] \tag{A13}
 \end{aligned}$$

$$\begin{aligned}
 & + \Gamma_8 \Gamma_7 E_3 \left[\frac{\wp^2}{2} (-s_3 - s_5 - E_3 h_1 - E_5 h_1 + 7\Delta (E_3 h_2 - E_5 h_2 + s_4 + s_6)) \right. \\
 & \left. + \wp \Delta \begin{pmatrix} 2 (E_3 h_2 - E_5 h_2 + s_4 + s_6) \\ +14\Delta (E_3 h_1 + E_5 h_1 + 2s_3 + 2s_5 + E_3 h_1 + E_5 h_1) \end{pmatrix} \right] \\
 S_7 = & \Gamma_6 \Gamma_7 E_5 \left[\frac{\wp^2}{2} (-r_1 - r_3 - E_3 s_1 - E_5 s_3 - E_3 s_5 + 7\Delta (r_4 - E_3 s_2 - E_5 s_4 + E_3 s_6)) \right. \\
 & \left. + \wp \Delta (-E_5 s_4 + E_3 s_6 - E_3 s_2 + r_4 + 7\Delta (r_1 + r_3 + E_3 s_5 + E_5 s_3)) \right] \\
 & + \Gamma_{10} \Gamma_7 \left[\frac{\wp^2}{2} (-E_3 r_3 - q_5 - E_5 r_1 + 7\Delta (q_6 + E_3 r_4)) \right. \\
 & \left. + 3\wp \Delta (q_6 + E_3 r_4) + 7\Delta (q_5 + E_5 r_1 + E_3 r_3) \right] \tag{A14}
 \end{aligned}$$

$$\begin{aligned}
 & + \Gamma_8 \Gamma_7 E_3 \left[\frac{\wp^2}{2} (-r_5 - E_3 s_1 - E_5 s_1 - r_3 + 7\Delta (r_4 + E_3 s_2 - E_5 s_2 + r_6)) \right. \\
 & \left. + \wp \Delta (2 (E_3 s_2 - E_5 s_2 + r_4 + r_6) + 14\Delta (r_3 + E_5 s_1)) \right] \\
 R_7 = & \Gamma_6 \Gamma_7 E_5 \left[\frac{\wp^2}{2} (-q_1 - E_3 r_1 - E_5 r_3 - E_3 r_5 + 7\Delta (q_2 - E_5 r_4 + E_3 r_6)) \right. \\
 & \left. + \wp \Delta (q_2 - E_5 r_4 + E_3 r_6 + 7\Delta (E_3 r_1 + E_5 r_3 + E_3 r_5 + q_1)) \right] \\
 & + \Gamma_{10} \Gamma_7 E_5 \left[\frac{\wp^2}{2} (-q_1 + 7\Delta q_2) + 3\wp \Delta (q_2 + 7\Delta q_1) \right] \tag{A15}
 \end{aligned}$$

$$\begin{aligned}
 & + \Gamma_8 \Gamma_7 E_3 \left[\frac{\wp^2}{2} (-q_5 - E_3 r_1 - E_5 r_1 + 7\Delta q_6) \right. \\
 & \left. + \wp \Delta (2 q_4 + 3 q_6 + 14\Delta (q_5 + E_3 r_1 + E_5 r_1)) \right] \\
 Z_7 = & \frac{\Gamma_6 \Gamma_7 E_5^2}{2} [\wp^2 (-z_3 - 7 z_4 \Delta) - 2\wp \Delta (z_4 + 7 z_3 \Delta)] \tag{A16}
 \end{aligned}$$

Where:

$$\Gamma_5 = \frac{1}{1 + 25\Delta^2}, \Gamma_6 = \frac{1}{g^2 + 4\Delta^2}, \Gamma_8 = \frac{1}{g^2 + 16\Delta^2}, \Gamma_{10} = \frac{1}{g^2 + 36\Delta^2} \quad (\text{A17})$$

$$\Gamma_1 = \frac{1}{1 + \Delta^2}, \Gamma_3 = \frac{1}{1 + 9\Delta^2}, \Gamma_7 = \frac{1}{2(1 + 49\Delta^2)} \quad (\text{A18})$$

$$f_5 = \frac{\Gamma_4 \Gamma_5 T_{3d} \Gamma_d}{64} \left[-\frac{\wp \alpha_3}{\Delta} + 20\alpha_3 \Delta + 2\wp^2 \alpha_4 \Delta + 8\wp \alpha_4 \Delta \right] \quad (\text{A19})$$

$$h_5 = E_3 \Gamma_5 \Gamma_d \left[\Gamma_2 T_{3d} \left(\frac{\wp \alpha_3}{32\Delta} + \frac{5\alpha_3 \Delta}{16} + \frac{\wp \alpha_4 \Delta}{8} + \frac{5\wp^2 \alpha_4 \Delta}{16} \right) + T_{1d} \left(\Gamma_4 \left(-\frac{\wp \alpha_1}{64\Delta} + \frac{5\alpha_1 \Delta}{16} + \frac{\wp \alpha_2 \Delta}{8} + \frac{5\wp^2 \alpha_2 \Delta}{32} \right) + \Gamma_2 \left(-\frac{\wp \alpha_1}{32\Delta} + \frac{5\alpha_1 \Delta}{16} + \frac{\wp \alpha_2 \Delta}{8} + \frac{5\wp^2 \alpha_2 \Delta}{16} \right) \right) \right] \quad (\text{A20})$$

$$s_5 = E_3^2 \Gamma_2 \Gamma_5 T_{1d} \Gamma_d \left[-\frac{\wp \alpha_1}{32\Delta} + \frac{5\alpha_1 \Delta}{16} - \frac{\wp \alpha_2 \Delta}{8} - \frac{5\wp^2 \alpha_2 \Delta}{16} \right] \quad (\text{A21})$$

$$r_5 = E_3 \Gamma_5 \Gamma_d \left[\Gamma_2 \left(-\frac{\wp}{8\Delta} - \frac{3\Delta}{2} - \frac{5\wp \Delta}{8} \right) + \Gamma_4 \left(-\frac{\wp}{16\Delta} - \frac{3\Delta}{2} - \frac{5\wp \Delta}{16} \right) \right] \quad (\text{A22})$$

$$q_5 = E_3^2 \Gamma_2 \Gamma_5 \Gamma_d \left(\frac{\wp}{8\Delta} - \Delta + \frac{5\wp \Delta}{8} \right) \quad (\text{A23})$$

$$f_6 = \Gamma_4 \Gamma_5 T_{3d} \Gamma_d \left(-\frac{\alpha_3}{16} - \frac{5\wp \alpha_3}{64} - \frac{\wp^2 \alpha_4}{32} + \frac{5\wp \alpha_4 \Delta^2}{8} \right) \quad (\text{A24})$$

$$h_6 = E_3 \Gamma_5 \Gamma_d \left(\Gamma_2 T_{3d} \left(-\frac{\alpha_3}{16} - \frac{5\wp \alpha_3}{32} - \frac{\wp^2 \alpha_4}{16} + \frac{5\wp \alpha_4 \Delta^2}{8} \right) + T_{1d} \left(\Gamma_2 \left(-\frac{\alpha_1}{16} - \frac{5\wp \alpha_1}{32} - \frac{\wp^2 \alpha_2}{16} + \frac{5\wp \alpha_2 \Delta^2}{8} \right) + \Gamma_4 \left(-\frac{\alpha_1}{16} - \frac{5\wp \alpha_1}{64} - \frac{\wp \alpha_2}{32} + \frac{5\wp \alpha_2 \Delta^2}{8} \right) \right) \right) \quad (\text{A25})$$

$$s_6 = E_3^2 \Gamma_2 \Gamma_5 T_{1d} \Gamma_d \left(-\frac{\alpha_1}{16} - \frac{5\wp \alpha_1}{32} + \frac{\wp^2 \alpha_2}{16} - \frac{5\wp \alpha_2 \Delta^2}{8} \right) \quad (\text{A26})$$

$$r_6 = E_3 \Gamma_5 \Gamma_d \left(\Gamma_4 \left(\frac{1}{4} + \frac{3\wp}{8} - \frac{5\Delta^2}{4} \right) + \Gamma_2 \left(\frac{1}{4} + \frac{3\wp}{4} - \frac{5\Delta^2}{4} \right) \right) \quad (\text{A27})$$

$$q_6 = E_3^2 \Gamma_2 \Gamma_5 \Gamma_d \left(\frac{1}{4} + \frac{\wp}{2} + \frac{5\Delta^2}{4} \right) \quad (\text{A28})$$

$$f_4 = \Gamma_d \Gamma_3 \left[\Gamma_2 \left(T_{1d} \left(-\frac{\alpha_1}{16} - \frac{3\wp \alpha_1}{32} - \frac{\wp^2 \alpha_2}{16} + \frac{3\wp \alpha_2 \Delta^2}{8} \right) + T_{3d} \left(-\frac{\alpha_3}{16} - \frac{3\wp \alpha_3}{32} - \frac{\wp^2 \alpha_4}{16} + \frac{3\wp \alpha_4 \Delta^2}{8} \right) \right) + \Gamma_4 T_{3d} \left(-\frac{\alpha_3}{16} - \frac{3\wp \alpha_3}{64} - \frac{\wp^2 \alpha_4}{32} + \frac{3\wp \alpha_4 \Delta^2}{8} \right) \right] \quad (\text{A29})$$

$$h_4 = T_{1d} \Gamma_d \Gamma_3 E_3 \left[\Gamma_2 \left(-\frac{\alpha_1}{16} - \frac{3\wp \alpha_1}{32} - \frac{3\wp \alpha_2 \Delta^2}{8} + \frac{\wp^2 \alpha_2}{16} \right) + \Gamma_4 \left(-\frac{\alpha_1}{16} - \frac{3\wp \alpha_1}{64} - \frac{\wp^2 \alpha_2}{32} - \frac{3\wp \alpha_2 \Delta^2}{8} \right) - \frac{3\alpha_1 \Delta}{8} \right] \quad (\text{A30})$$

$$s_4 = \Gamma_3 \Gamma_d \left[\Gamma_2 \left(\frac{1}{4} + \frac{\wp}{2} - \frac{3\Delta^2}{4} \right) + -\frac{3E_3^2 T_{3d} \alpha_3 \Delta}{8} \right] \quad (\text{A31})$$

$$r_4 = \Gamma_3 \Gamma_d E_3 \left[\frac{\Gamma_3 \Gamma_d}{4} (1 + \wp + 3\Delta^2) + \left(\frac{\Gamma_4}{4} (1 + \wp - 3\Delta^2) + \frac{3\Delta}{2} \right) \right] \quad (\text{A32})$$

$$z_4 = -3E_3 \Gamma_3 \Delta \quad (\text{A33})$$

$$f_3 = \Gamma_3 \Gamma_d \left[\begin{array}{l} \Gamma_2 \left(T_{1d} \left(-\frac{\varphi \alpha_1}{32\Delta} + \frac{3\alpha_1\Delta}{16\Delta} + \frac{\varphi \alpha_2\Delta}{8} + \frac{3\varphi^2\alpha_2\Delta}{16} \right) \right) \\ + T_{3d} \left(-\frac{\varphi \alpha_3}{32\Delta} + \frac{\varphi \alpha_4\Delta}{8} + \frac{3\varphi^2\alpha_4\Delta}{16} + \frac{3\alpha_3\Delta}{16} \right) \\ + \Gamma_4 T_{3d} \left(\frac{3\alpha_3\Delta}{16} - \frac{\varphi \alpha_3}{64\Delta} + \frac{\varphi \alpha_4}{8} + \frac{3\varphi^2\alpha_4\Delta}{32} \right) \end{array} \right] \quad (\text{A34})$$

$$h_3 = \Gamma_3 \Gamma_d T_{1d} E_3 \left[\begin{array}{l} \Gamma_2 \left(-\frac{\varphi \alpha_1}{32\Delta} + \frac{3\alpha_1\Delta}{16} - \frac{\varphi \alpha_2\Delta}{8} - \frac{3\varphi^2\alpha_2\Delta}{16} \right) \\ + \Gamma_4 \left(\frac{\varphi \alpha_2\Delta}{8} + \frac{3\varphi^2\alpha_2\Delta}{32} - \frac{\varphi \alpha_1}{64\Delta} + \frac{3\alpha_1\Delta}{16} \right) - \frac{\alpha_1}{8} \end{array} \right] \quad (\text{A35})$$

$$s_3 = \Gamma_3 \Gamma_d \left[-\frac{E_3^2 T_{3d} \alpha_3}{8} + \Gamma_2 \left(\frac{\varphi}{8\Delta} - \frac{3\varphi\Delta}{8} - \Delta \right) \right] \quad (\text{A36})$$

$$r_3 = \Gamma_3 \Gamma_d E_3 \left[\frac{1}{2} + \Gamma_2 \left(\frac{\varphi}{8\Delta} - \frac{\Delta}{2} + \frac{3\varphi\Delta}{8} \right) + \Gamma_4 \left(-\frac{3\Delta\varphi}{16} + \frac{\varphi}{16\Delta} - \Delta \right) \right] \quad (\text{A37})$$

$$z_3 = -E_3 \Gamma_3 \quad (\text{A38})$$

$$f_2 = \Gamma_1 \Gamma_d \left[\begin{array}{l} \Gamma_2 \left(T_{1d} \left(-\frac{\alpha_1}{16} - \frac{\varphi \alpha_1}{32} + \frac{\varphi \alpha_2\Delta^2}{8} - \frac{\varphi^2\alpha_2}{16} \right) \right) \\ + T_{3d} \left(-\frac{\alpha_3}{16} - \frac{\varphi \alpha_3}{32} - \frac{\varphi^2\alpha_4}{16} + \frac{\varphi \alpha_4\Delta^2}{8} \right) \end{array} \right] - \frac{T_{1d}\alpha_1\Delta}{8} \quad (\text{A39})$$

$$h_2 = \Gamma_1 \Gamma_d E_3 \left[\begin{array}{l} \Gamma_2 \left(T_{1d} \left(-\frac{\varphi \alpha_1}{16} + \frac{\varphi^2\alpha_2}{8} \right) + \right. \\ \left. T_{3d} \left(\frac{\alpha_3}{16} - \frac{\varphi \alpha_3}{32} + \frac{\varphi^2\alpha_4}{16} + \frac{\varphi \alpha_4\Delta^2}{8} \right) \right) \\ + T_{3d} \left(\Gamma_4 \left(-\frac{\alpha_3}{16} - \frac{\varphi \alpha_3}{64} - \frac{\varphi^2\alpha_4}{32} + \frac{\varphi \alpha_4\Delta^2}{8} \right) - \frac{\Gamma_3\alpha_3\Delta}{8} \right) \end{array} \right] \quad (\text{A40})$$

$$s_2 = \Gamma_1 \Gamma_d \left[\begin{array}{l} \Gamma_2 \left(\frac{1}{4} + \frac{\gamma}{4} + T_{1d} \left(E_3^2 \left(-\frac{\alpha_1}{16} - \frac{\varphi \alpha_1}{32} - \frac{\varphi^2\alpha_2}{16} - \frac{\varphi \alpha_2\Delta^2}{8} \right) \right) \right) \\ - \frac{\Delta^2}{4} \end{array} \right] + \Gamma_4 T_{1d} E_3^2 \left(-\frac{\alpha_1}{16} - \frac{\varphi \alpha_1}{64} - \frac{\varphi^2\alpha_2}{32} + \frac{\varphi \alpha_2\Delta^2}{8} \right) + \frac{\Delta}{2} \quad (\text{A41})$$

$$q_2 = \Gamma_1 \left[\Gamma_d E_3^2 \left(\Gamma_2 \left(-\frac{1}{4} + \frac{\varphi}{4} - \frac{\Delta^2}{4} \right) + \Gamma_4 \left(\frac{1}{4} + \frac{\varphi}{8} - \frac{\Delta^2}{4} \right) \right) - \Delta \right] \quad (\text{A42})$$

$$f_1 = \Gamma_1 \Gamma_d \left[-\frac{T_{1d}\alpha_1}{8} + \Gamma_2 \left(T_{1d} \left(-\frac{\varphi \alpha_1}{32\Delta} + \frac{\alpha_1\Delta}{16} + \frac{\varphi \alpha_2\Delta}{8} + \frac{\varphi^2\alpha_2\Delta}{16} \right) \right) \right. \\ \left. + T_{3d} \left(\frac{\alpha_3\Delta}{16} + \frac{\varphi \alpha_4\Delta}{8} + \frac{\varphi^2\alpha_4\Delta}{16} - \frac{\varphi \alpha_3}{32\Delta} \right) \right] \quad (\text{A43})$$

$$h_1 = \Gamma_1 \Gamma_d E_3 \left[\begin{array}{l} \Gamma_2 \left(T_{1d} \left(-\frac{\varphi \alpha_1}{16\Delta} - \frac{\varphi^2\alpha_2\Delta}{8} \right) + \right. \\ \left. T_{3d} \left(-\frac{\varphi \alpha_3}{32\Delta} - \frac{\alpha_3\Delta}{16} + \frac{\varphi \alpha_4\Delta}{8} - \frac{\varphi^2\alpha_4\Delta}{16} \right) \right) \\ + \Gamma_4 T_{3d} \left(\frac{\varphi^2\alpha_4\Delta}{32} - \frac{\varphi \alpha_3}{64\Delta} + \frac{\alpha_3\Delta}{16} + \frac{\varphi \alpha_4\Delta}{8} \right) - \frac{\alpha_3 T_{3d}}{8} \end{array} \right] \quad (\text{A44})$$

$$s_1 = \Gamma_1 \Gamma_d \left[\begin{array}{l} \Gamma_2 \left(\frac{\varphi}{8\Delta} - \frac{\Delta}{2} - \frac{\varphi\Delta}{8} + \right. \\ \left. T_{1d} E_3^2 \left(-\frac{\varphi \alpha_1}{32\Delta} - \frac{\alpha_1\Delta}{16} - \frac{\varphi \alpha_2\Delta}{8} + \frac{\varphi^2\alpha_2\Delta}{16} \right) \right) \\ + \Gamma_4 T_{1d} E_3^2 \left(\frac{\varphi \alpha_2\Delta}{8} + \frac{\varphi^2\alpha_2\Delta}{32} - \frac{\varphi \alpha_1}{16\Delta} + \frac{\alpha_1\Delta}{16} \right) + \frac{1}{2} \end{array} \right] \quad (\text{A45})$$

$$r_1 = \frac{\Gamma_1 \Gamma_2 \Gamma_d E_3}{4} \varphi \left[\frac{1}{\Delta} + \Delta \right] \quad (\text{A46})$$

$$q_1 = \Gamma_1 \left[-1 + \Gamma_d E_3^2 \left(\Gamma_2 \left(\frac{\varphi}{8\Delta} + \frac{\Delta}{2} - \frac{\varphi\Delta}{8} \right) + \Gamma_4 \left(\frac{\varphi}{16\Delta} - \frac{\Delta}{2} - \frac{\varphi\Delta}{16} \right) \right) \right] \quad (\text{A47})$$